IMPLEMENTATION OF LOAD-PATH TOPOLOGY OPTIMISATION IN SAMCEF FOR THE GENERATION OF COMPLIANT STRUCTURES

M.J. SANTER S. PELLEGRINO

Department of Engineering,
University of Cambridge,
Trumpington Street, Cambridge.
CB2 1PZ, UK

Abstract : *An implementation of load-path topology optimisation is presented which enables the synthesis of lattice-based compliant structures (with both distributed and concentrated compliance) using the existing functionality of SAMCEF and BOSS-quattro. A case study concerning the design of a compliant aircraft wing leading edge is used to illustrate the technique and to demonstrate how the logical program flow available in the SAMCEF command language may be used to enable the optimisation algorithms to vary structural topology in addition to the geometry. Ways of extending the method for more complex optimisation problems are discussed.*

1 INTRODUCTION

This paper will demonstrate the implementation of a technique for the topology and geometry optimisation of lattice-based structures for use with SAMCEF and BOSS-quattro. This technique incorporates nonlinear finite element analysis (FEA) with Genetic Algorithms (GAs). The approach makes strong use of the existence of basic logical flow within the SAMCEF command language to enable the GA to explore a large potential design space from a suitably-parameterised starting configuration.

As a means of illustrating this technique, a case study consisting of the generation of a compliant aircraft rib leading-edge is used. This case study demonstrates how, by using the method, an adaptive structure may be designed for complex load cases and geometrically nonlinear behaviour.

1.1 COMPLIANT STRUCTURES

Central to the purpose of the optimisation is the creation of compliant structures. These are structures which undergo potentially large deformations under actuation, and which may be considered to approximate the functionality of mechanisms [1,3]. For example the behaviour of a rotational hinge may be approximated by a localised region of reduced thickness, and consequently substantially reduced bending stiffness, known as a living hinge.

There are many advantages to using compliant structures instead of conventional mechanisms. A major benefit, for example, is that compliant structures may be constructed as single monolithic entities, which may result in substantial reductions in component assembly time. In addition, maintenance requirements such as the need to provide lubrication in a conventional hinge, are reduced or removed, and the structure itself may be suitable for applications in environments that are ill-suited to mechanisms. An example of a system for which the use of compliant structures provides a substantial benefit is shown in Fig. 1. This is a compliant wing

trailing edge, developed by FlexSys Inc. In this example, the use of a compliant structure replicates the behaviour of a trailing-edge flap, with the difference that the deformed shape still has a continuous profile. This continuity has substantial aerodynamic benefits resulting in reduced turbulence and improved efficiency [2].

A structure whose compliance is localised in small regions (such as a living hinge) is said to exhibit concentrated (or lumped) compliance [5]. Alternatively, a structure may deform in a less localised fashion, in other words due to flexure of the entire structure, in which case it is said to exhibit distributed compliance.

Many analysis techniques are currently available for compliant structures. For example, structures with concentrated compliance may be approximated by pseudo-rigid-body models [1]. In this case, the regions of concentrated compliance are represented by pin-joints (possibly including torsional springs to represent the restoring moments resulting from flexure of living hinges), and the stiffer regions of the structure by rigid elements. The behaviour of structures with distributed compliance, however, is usually more complex, and is intractable to classical analysis in all but the simplest cases. In this case FEA must be used.

The complex, and sometimes unintuitive behaviour of compliant structures means that their design is not straightforward. In particular, the optimum solution for a given design specification is difficult to determine. For this reason the use of computational optimisation is particularly attractive as it enables a design to be generated which is the optimum solution for a given set of design specifications, when limited or no information is available concerning the most suitable structural topology or geometry.

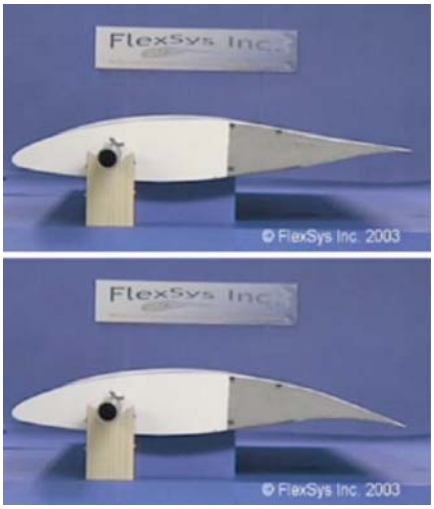

Fig. 1 An aircraft wing with a compliant trailing edge © Flexsys Inc. 2003

1.2 OUTLINE OF PAPER

Subsequent to this Introduction, this paper will first describe the case study that will be used to illustrate the developed techniques. This is a concept for a lattice-based adaptive aircraft wing rib, similar to the example shown in Fig. 1, which, when coupled with the wing skin forms a compliant structure. Under a single displacement actuation, the shape change of the combined compliant structure produces the effect of a leading-edge flap.

Following this, the definition of the SAMCEF finite element model and the necessary parameterisation for the BOSS-quattro optimisation algorithm will be presented. In addition, particular attention will be given to the implementation of the optimisation technique using the SAMCEF command language. The optimum structure suggested by an initial optimisation analysis is then taken further and corrected to ensure that maximum stresses are not exceeded in addition to the desired shape change being achieved. It is noted that the maximum stresses are concentrated in the compliant rib structure and not the wing skin, so a demonstration model which does not include the wing skin is designed and constructed. Finally suggestions are made for possible improvements to the optimisation and conclusions are drawn. All work presented in this paper used SAMCEF v.12.0-03, and BOSS-quattro v.6.0-01.

2 ADAPTIVE WING CASE STUDY

The case study presented in this paper is for an adaptive aircraft wing leading edge, suitable for incorporation into a design for an Unmanned Aerial Vehicle (UAV). Its design was investigated by the authors in collaboration with Alenia-Aeronautica and Samtech within the Synthesis of Compliant Mechanical Systems (SYNCOMECS) project.

2.1 ADAPTIVE WING DESCRIPTION

The wing profile specified by Alenia is the NACA-2421 profile with a chord length of 1056 mm. The leading edge was defined as the first 25% of the chord length *c*. The rib has a fixed depth of 5 mm and the spacing between consecutive ribs in the wing spanwise direction is 250 mm. The leading edge (shown in the context of a complete wing section for comparison with Fig. 1) is illustrated in Fig. 2. The wing skin has a uniform thickness of 1 mm, and in addition the rib is connected to the skin by means of a 1 mm thick and 5 mm wide strip. The rib-connection strip is represented in Fig. 2 by thin lines offset both sides of curve AB. The actuation resulting in the shape change of the compliant structure is a 10 mm displacement applied at a single point on the vertical axis at the ¼-chord (represented by line AB in Figs. 2 and 3.)

The compliant rib structure is chosen to have a lattice form i.e. to consist of a network of beam members. Accordingly they are modelled with beam elements. The skin and the rib-skin connection strip are modelled with shell elements. Boundary conditions are applied such that the skin is fully fixed along lines CD and EF (defined in Fig. 2) and restrained against spanwise (z-direction) deflection at the two remaining free edges – curves CE and DF. In addition to the displacement actuation, aerodynamic pressure loading is applied to the skin. This pressure is taken as that resulting from an air speed of 260 kts (134 m/s) at sea level at 5º angle of attack, assuming an inviscid flow. Although in reality, a change in wing profile would alter this pressure loading, this effect is not considered, and the pressure load is assumed to remain constant. To assume otherwise would require a full aeroelastic analysis which is beyond the scope of this paper.

2.2 OPTIMISATION PROBLEM DEFINITION

It is useful to break a topology optimisation problem down into a number of constituent components as follows. First, it is necessary to define the design space. This is the region of (two- or three-dimensional) space within which all generated structure must be confined. In the case of the adaptive aircraft wing the design space

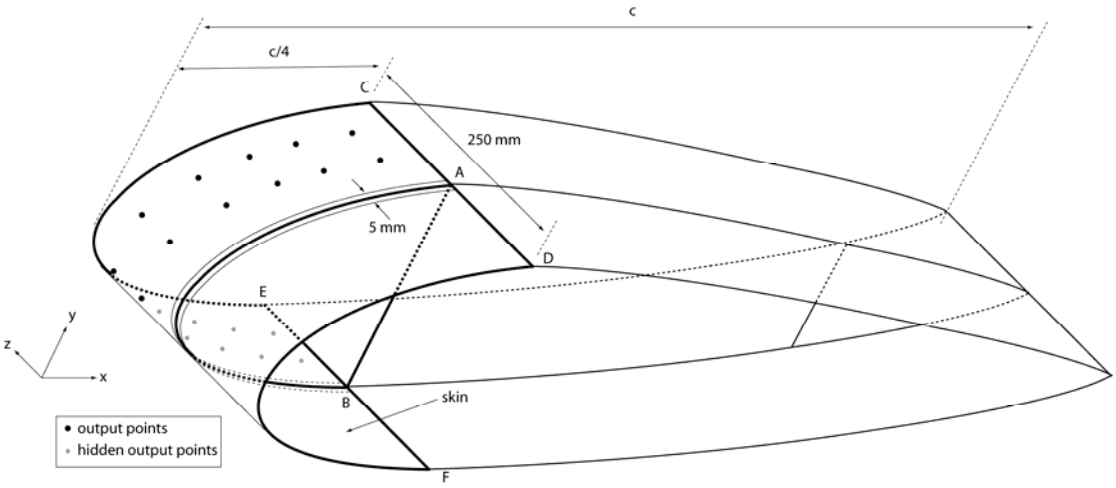

Fig. 2 Adaptive wing optimisation problem definition (1) – geometry and output points

(shown in Fig. 3) is determined by the wing profile itself, which is defined by the area bounded by line AB and curve AB – evidently all wing structure must be contained within the skin.

Second, control points, through which any generated structure must pass, must be defined. These may be fixed in space, for example corresponding to required attachment points, or they may be free to float within the design space. In the latter case, this enables the geometry to be optimised in addition to the topology. In the aircraft wing there are six control points which are permitted to move through the design space subject to additional constraints which are described below. Additionally, there are nine control points which provide attachment points between the rib structure and the wing skin, boundary of the design space and which are constrained to lie on the design space boundary. These are shown in Fig. 3.

Third, input and output points, the former corresponding to locations where loads and displacements are applied, and the latter being locations at which the desired shape change of the wing profile is measured, are included. They may be fixed or free to move within the design space. In the aircraft wing there is a single input point, labelled 7 in Fig. 3, constrained to lie on line AB, at which the displacement actuation is applied –. The aerodynamic loading is applied to the wing profile boundary. The output points, at which the deflection of the wing skin under actuation and aerodynamic loading is measured, are shown on the wing surface in Fig. 2.

The material properties assumed throughout are those of High Strength Aluminium and are tabulated in Table 1. An isotropic material model is used.

Young's Modulus E (N/mm^2)	72,000
Poisson's Ratio ν	0.33
Yield Strength σ_Y (N/mm^2)	395

Table 1. Material properties of High Strength Aluminium

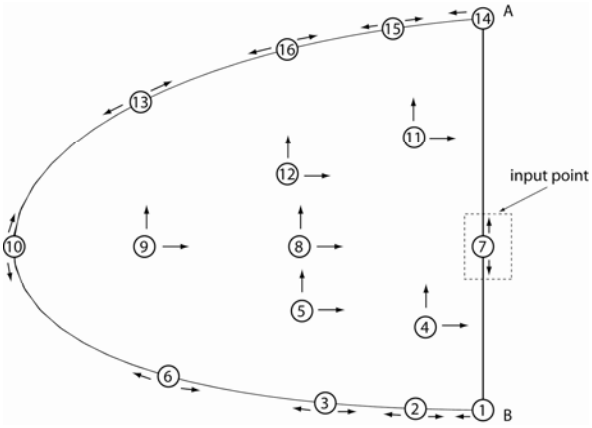

Fig. 3 Adaptive wing optimisation problem definition (2) – design space, input and output points

2.2.1 Load-Path Optimisation

In order to generate a lattice-based structure using computational optimisation it is necessary to provide a starting point in the form of a parent lattice which contains all possible members. Such a parent lattice is shown for the adaptive wing case study in Fig. 4. In order to be able to generate different topologies the optimisation algorithm must to be able to remove members whilst retaining a fully-connected structure. A possible technique for doing this is to assign a binary parameter to each member (where '1' corresponds to 'member exists' and '0' to 'member does not exist')[3]. This is an acceptable approach when gradient-based optimisation algorithms are used. There are, however, many good reasons why a GA optimisation is to be preferred when synthesising compliant structures. In particular, they explore the full design space irrespective of starting point, and they are less likely than gradient-based algorithms to converge to a local minimum.

If, however, GAs are used in conjunction with the member parameterisation scheme described above, there is a strong likelihood of disconnected structures being generated which results in FEA errors causing the optimisation in BOSS-quattro to stop. It is therefore necessary to determine an alternative member-parameterisation scheme to insure that every GA iteration is guaranteed to produce a valid structure.

The technique proposed in [4] is to assign a binary parameter, not to the existence of a single member, but to the existence of a sequence of members forming a load path. It is shown in [4] that provided there is at least one load-path between the inputs and the outputs, the inputs and the ground, and the outputs and the ground, a valid structure will be generated. This is the parameterisation strategy used for the topological optimisation of the adaptive wing rib. However, only the first of these three conditions must be satisfied in the present case, as the wing skin and rib-skin connection strip guarantees the connection to ground.

An example of how switching load paths on and off can provide different structural topologies is provided in Fig. 5. In this figure, the structure consists of the superposition of four load paths connecting the points as follows: [7 8 4 1], [7 8 9 6], [7 8 9 10], and [7 11 15]. It should be noted that the determination of the load paths for many parent lattices is not a straightforward task. However, for the purposes of this paper, the relevant load paths are assumed to have been determined.

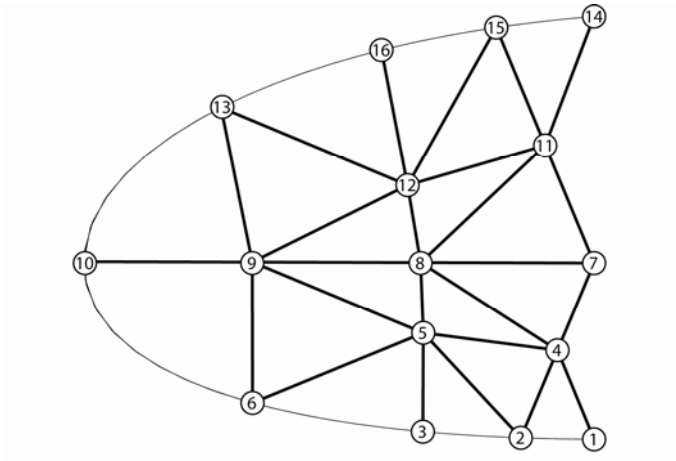

Fig. 4 Parent lattice illustration

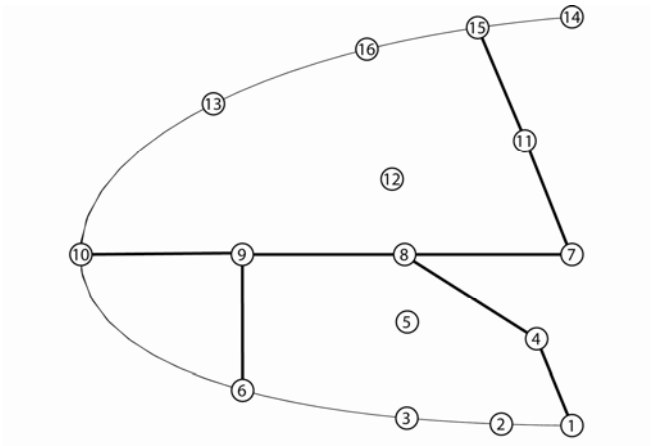

Fig. 5 Example topology generated using 5 load paths

2.3 GENERATION OF FEASIBLE STRUCTURES

Use of the load-path parameterisation technique, described in Section 2.2.1, ensures that valid structures, from a mathematical point of view, are generated. It is also necessary, however, to ensure that the structures are feasible from a physical perspective, in other words, can be constructed.

The most likely reason for a structure generated by a GA to be physically impossible to construct is that two or more members may cross over each other. This may be in part avoided by choosing a parent lattice which does not contain any crossing members. However, if the internal control points are free to move within the design space it is possible for cross-over to occur even if it is not present in the parent lattice, as shown in Fig. 6. In this case it is necessary to constrain the movement of the control points whilst still ensuring that as much of the design space as possible can be explored by the GA.

This movement restriction is implemented by parameterising all the control points' movement in terms of the displacement, expressed in polar coordinates, from their starting configuration. The angle need not be controlled, but the radius must be limited to prevent cross-over. To do this, each control point is assigned a boundary domain which is defined by a polygon of points surrounding it. This is shown in Fig. 7. The maximum radius that a control point may move in a particular iteration is

determined by the smallest perpendicular distance of the control point from edges of the polygon defining its boundary domain. Referring to Fig. 7, this radius is equal to

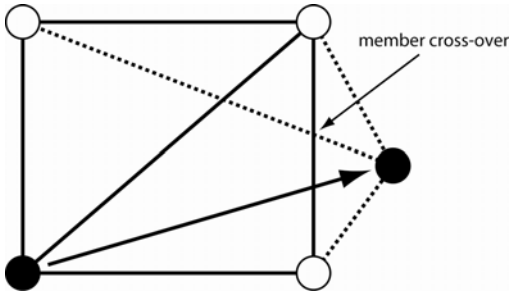

Fig. 6 Illustration of control point movement resulting in member cross-over

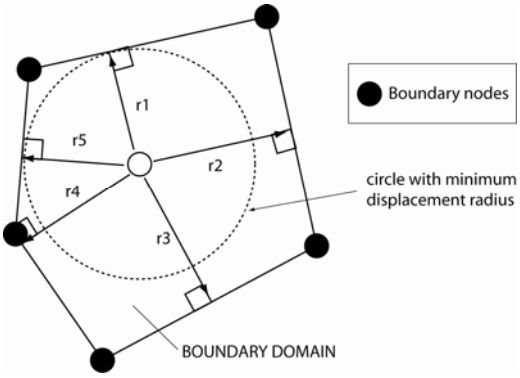

Fig. 7 Removal of the possibility of member cross-over using nodal boundary domains

min(r1,r2,r3,r4,r5). The implementation of this approach using the SAMCEF command language is described in the following section.

3 MODEL PARAMETERISATION

In this section a detailed description of the parameterisation and automatic meshing of the adaptive wing leading edge within SAMCEF is presented. The SAMCEF commands that implement each part of the scheme are shown in boxes. This section consists of three parts. The first considers the generation of the underlying geometry of the adaptive wing, including the implementation of the anti-cross-over scheme. This is followed by an illustration of how the correct members may be meshed, depending on which load paths are switched on. Finally it is demonstrated how the connections between adjacent members may be parameterised to be either rigid or hinged. This makes the optimisation process extremely powerful as it allows structures with both distributed and concentrated compliance to be synthesised.

3.1 GENERATION OF BASE GEOMETRY

The base geometry for the wing skin and rib-skin connection strip are known from the beginning and are unchanged by the optimisation. Only the underlying geometry for the compliant rib members is varied. In the following, the point numbers are those defined in Fig. 4.

The first point that is placed corresponds to the location of the actuation displacement. Its x-coordinate is fixed, but the y-coordinate is parameterised to vary between the upper and the lower wing surfaces.

```
ABRE '/point7y' '0.0'

.3POINT
I 1007 X 264.0 Y (/point7y) Z 0.0
```

Once the actuation point is placed, the points at which the rib members connect to the rib-skin connection strip are then determined. This is carried out by projecting from the actuation point (7) onto the surface defining the wing profile (and which forms the basis for the wing skin mesh) at prescribed angles. In fact, the angles are not directly parameterised as this would mean that extra constraints would have to be introduced in the optimisation to ensure that the sum of all the angles never exceeds 180º. This is to ensure that all points remain within the design space i.e. inside the leading edge. Instead the parameter associated with each point corresponds to the percentage of the remaining available angle. This ensures that the attachment points always remain within the leading edge. This parameter is defined as '/fac*n*' for attachment point *n*.

```
ABRE '/ang14' '(180*/fac14)'
ABRE '/ang15' '(/ang14+/fac15*(180-/ang14))'
ABRE '/ang16' '(/ang15+/fac16*(180-/ang15))'
ABRE '/ang13' '(/ang16+/fac13*(180-/ang16))'
ABRE '/ang10' '(/ang13+/fac10*(180-/ang13))'
ABRE '/ang06' '(/ang10+/fac06*(180-/ang10))'
ABRE '/ang03' '(/ang06+/fac03*(180-/ang06))'
ABRE '/ang02' '(/ang03+/fac02*(180-/ang03))'
ABRE '/ang01' '(/ang02+/fac01*(180-/ang02))'

.3POINT
I 14 PROJETER 7 SURFACE 1 DIRECTION (-sin(/ang14)) (cos(/ang14)) 0
I 15 PROJETER 7 SURFACE 1 DIRECTION (-sin(/ang15)) (cos(/ang15)) 0
I 16 PROJETER 7 SURFACE 1 DIRECTION (-sin(/ang16)) (cos(/ang16)) 0
I 13 PROJETER 7 SURFACE 1 DIRECTION (-sin(/ang13)) (cos(/ang13)) 0
I 10 PROJETER 7 SURFACE 1 DIRECTION (-sin(/ang10)) (cos(/ang10)) 0
I  6 PROJETER 7 SURFACE 1 DIRECTION (-sin(/ang06)) (cos(/ang06)) 0
I  3 PROJETER 7 SURFACE 1 DIRECTION (-sin(/ang03)) (cos(/ang03)) 0
I  2 PROJETER 7 SURFACE 1 DIRECTION (-sin(/ang02)) (cos(/ang02)) 0
I  1 PROJETER 7 SURFACE 1 DIRECTION (-sin(/ang01)) (cos(/ang01)) 0
```

At this point it is necessary to store the coordinates of the newly created points as additional variables by means of the #INQ command, for example

```
#INQ (/point15x, POINT, 15, X)
#INQ (/point15y, POINT, 15, Y)
```

to enable the remaining control points to be inserted. Although their coordinates are parameterised and may therefore vary, as a starting point they are placed at pre-defined locations. This provisional placement (again shown in Fig. 4) is based on the rays that were used to project the attachment point locations.

```
.3POINT
I  4 X (/point2x+0.5*(/point7x-/point2x))    Y (/point2y+0.5*(/point7y-/point2y))    Z 0.0
I  5 X (/point6x+0.5*(/point7x-/point6x))    Y (/point6y+0.5*(/point7y-/point6y))    Z 0.0
I  8 X (/point10x+0.66*(/point7x-/point10x)) Y (/point10y+0.66*(/point7y-/point10y)) Z 0.0
I  9 X (/point10x+0.33*(/point7x-/point10x)) Y (/point10y+0.33*(/point7y-/point10y)) Z 0.0
I 12 X (/point13x+0.5*(/point7x-/point13x))  Y (/point13y+0.5*(/point7y-/point13y))  Z 0.0
I 11 X (/point15x+0.5*(/point7x-/point15x))  Y (/point15y+0.5*(/point7y-/point15y))  Z 0.0
```

Having temporarily placed the control points within the design space, further parameterisation enables their positions to be varied. First the x- and y-coordinates of all of the points are stored as variables using the #INQ function and further abbreviations are defined which enable the determination of the control point boundary domain radii. An illustration of this for control point 4, whose boundary points are 1, 2, 5, 7 and 8, is given below.

```
ABRE '/b4a' '(SQR(((/point4x-/point1x)**2+(/point4y-/point1y)**2)-$
(((((/point4x-/point1x)*(/point2x-/point1x)+$
(/point4y-/point1y)*(/point2y-/point1y))**2):$
((/point2x-/point1x)**2+(/point2y-/point1y)**2))))'
ABRE '/b4b' '(SQR(((/point4x-/point2x)**2+(/point4y-/point2y)**2)-$
(((((/point4x-/point2x)*(/point5x-/point2x)+$
(/point4y-/point2y)*(/point5y-/point2y))**2):$
((/point5x-/point2x)**2+(/point5y-/point2y)**2))))'
ABRE '/b4c' '(SQR(((/point4x-/point5x)**2+(/point4y-/point5y)**2)-$
(((((/point4x-/point5x)*(/point8x-/point5x)+$
(/point4y-/point5y)*(/point8y-/point5y))**2):$
((/point8x-/point5x)**2+(/point8y-/point5y)**2))))'
ABRE '/b4d' '(SQR(((/point4x-/point8x)**2+(/point4y-/point8y)**2)-$
(((((/point4x-/point8x)*(/point7x-/point8x)+$
(/point4y-/point8y)*(/point7y-/point8y))**2):$
((/point7x-/point8x)**2+(/point7y-/point8y)**2))))'
ABRE '/b4e' '(SQR(((/point4x-/point7x)**2+(/point4y-/point7y)**2)-$
(((((/point4x-/point7x)*(/point1x-/point7x)+$
(/point4y-/point7y)*(/point1y-/point7y))**2):$
((/point1x-/point7x)**2+(/point1y-/point7y)**2))))'
```

At this point the positions of the control points are modified in sequence according to their position parameters. For control point *n* these are the polar coordinate angle '/point*n*q' and the proportion of the minimum boundary domain radius that will be used. The re-definition of the location of control point 4 is now illustrated.

```
.3POINT
I 4 X (/point4x+/point4r*(MIN(/b4a,/b4b,/b4c,/b4d,/b4e))*cos(/point4q)) $
    Y (/point4y+/point4r*(MIN(/b4a,/b4b,/b4c,/b4d,/b4e))*sin(/point4q)) Z 0
.SEL
#INQ (/point4x, POINT, 4, X)
#INQ (/point4y, POINT, 4, Y)
```

It can be seen that, following repositioning, the control point's new coordinates are stored. This means that all subsequent control point modifications are made with reference to the updated configuration. The control points are then connected with lines (.3DROIT). At this stage all of the base geometry is in place and the model may be meshed.

3.2 MESHING OF SWITCHED-ON MEMBERS

The first step is to mesh the skin and the rib-skin connection strip. In order to ensure that a connection is possible between a member and the connection strip, the contour definition for the strip includes the connection points. This ensures that a node is placed at these locations by the automatic mesher.

In order to mesh the required rib structure, it is necessary to associate the load paths with each member. By way of example, here member 1 (connecting points 1 and 4) is associated with load paths 1,2,3 … 9,10. Recalling that a binary parameter is used to determine the existence of a particular load path, with '1' representing 'load path exists', a member must be meshed if any of its associated load path parameters is equal to one.

```
#IF (MAX(/p1,/p2,/p3,/p4,/p5,/p6,/p7,/p8,/p9,/p10) EQ 1) THEN
ABRE '/member01_exists' '1'
.GEN
MAILLE 1 LIGNE
.SEL
GROUP NOM "connect_01" MAILLES LIGNE 1
.BEA GROUP "connect_01" DIRECTION 0 0 1
.BPR NOM "prof_01" UNIT 0.001 TYPE "RECT" B (/thickness01) H (/beam_depth)
.AEL GROUP "connect_01" MAT "Aluminium" PROFILE "prof_01"
#ENDIF
```

It can be seen that at this stage the cross-sections of the connection members are also defined via thickness and depth parameters. Additionally the existence of a particular member is recorded by means of a further abbreviation, which is used to speed up the pre-processor, by ensuring that only connection types for existing members are determined.

3.3 DETERMINATION OF CONNECTION TYPE

Once all the required rib members have been meshed, the final stage of the model generation is to provide connections between them. At the current time these connections are permitted to be either rigid or pinned (defined by means of the .MCE/.MCC commands), and are determined by two parameters for each member – one for each end. For member 1 the connection type at the two ends ‘a’ and ‘b’ are stored as ‘/c_01a’ and ‘/c01b’ respectively.

A master node is placed at each connection point to act as the hub for all the members that connect to it. (As can be seen below, a high node number is chosen to ensure that it has not already been used by the automatic mesher.) It can be seen that where members meet at a hub there will be several coincident nodes – the master node and all the end nodes of the concurrent members. In order to ensure that the correct connection type is associated with the correct member it is first necessary to isolate the node numbers corresponding to the ends of the current member, and to save them as abbreviations. The isolation is carried out by means of Boolean operations on groups of nodes. For example, a group is defined which contains all the nodes at a particular hub. Then a second group is defined which contains all the nodes of a particular member. The end node of the member may be isolated by taking the intersection of these two groups. To save computer time the operations are only carried out if the member is found to have been meshed.

```
.NOE
I 100004 POINT 4

#IF (/member01_exists EQ 1) THEN
.SEL
GROUP NOM "nodes1" NOEUDS POINT 1
GROUP NOM "nodes4" NOEUDS POINT 4
GROUP NOM "nodes_m01" NOEUDS LIGNE 1
GROUP NOM "node_01_a" IDENTIQUE "nodes_m01" "nodes1"
GROUP NOM "node_01_b" IDENTIQUE "nodes_m01" "nodes4"
SUPPR GROUP "nodes1"
SUPPR GROUP "nodes4"
.NOE
#INQ(/N1a,GR,"con_node1",S1)
#INQ(/N2a,GR,"node_01_a",S1)
#INQ(/N2b,GR,"node_01_b",S1)
#IF (/c_01a EQ 0) THEN
.MCE GP "m01_n1" RIGI N (/N1a) (/N2a)
#ELSEIF (/c_01a EQ 1) THEN
.MCE GP "m01_n1" HING N (/N1a) (/N2a)
.MCC GP "m01_n1" HING AXE1 3
#ENDIF
```

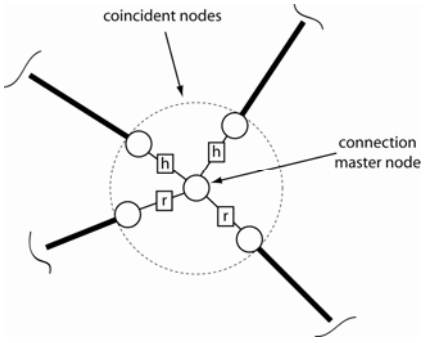

Fig. 8 Different connection types at an intersection of 4 members

```
#IF (/c_01b EQ 0) THEN
.MCE GP "m01_n4" RIGI N 100004 (/N2b)
#ELSEIF (/c_01b EQ 1) THEN
.MCE GP "m01_n4" HING N 100004 (/N2b)
.MCC GP "m01_n4" HING AXE1 3
#ENDIF
#ENDIF
```

A sketch of how the different connection types are meshed to a hub formed by a master node is shown in Fig. 8, with ‘h’ representing a hinge, and ‘r’ a rigid connection.

At this point the parameterisation of the model is complete and it only remains to apply the boundary conditions, the actuation displacement and the pressure loading into the analysis file.

4 OPTIMISATION EXAMPLE

4.1 OPTIMISATION DESCRIPTION

The SAMCEF model described in the preceding section is fully-parameterised to include the possibility of variable rib member cross-sections and variable member connection types in addition to the topology and configuration of the compliant rib structure.

However, in order to speed up the convergence of the optimisation, the first example given below has the model parameterisation restricted to the topology and configuration of the rib structure only. All member cross-sections are fixed at 5 mm wide and 5 mm deep, and all connections are rigid. This means that localised compliance is not permitted in the resulting compliant structure.

It is necessary for the model to be analysed using the MECANO module in order to be able to account for the hinge elements. However, because the expected deflections are small, and in order to speed up the analysis, it is linearised using the ‘.SAM NLIS -1’ command. This substantially improves the optimisation time. Following the optimisation, it was found that, in the case of the adaptive wing, provided no members buckle, the displacements are such that a linear analysis is sufficient to capture the behaviour under actuation.

The GA chosen for BOSS-quattro was ‘Evolution_JCO_real’. The topology is represented by 90 possible load paths. The population size is 10 individuals and all options were maintained at their default settings with the exception that rebirth was permitted. This is to enable more of the design space to be explored, which is useful when the problem is not well-understood at the beginning.

In the initial optimisation, no constraints were applied – it was intended to reduce the peak stress in a subsequent step. Two equally-weighted objectives were set for the optimisation, the ‘model-complexity’ and the ‘rms-error’ which are described in detail below.

In the context of the adaptive wing, a desirable solution is one that minimises the mass. However, as large numbers of load paths can be associated with a particular member, this means that switching a single load path off is unlikely to have a significant effect on the structural mass. Instead the parameter that is minimised is the ‘model-complexity’ which in this case is equal to the number of active load paths. As will be shown in a Section 6 this definition may be extended to include, for example, the number of hinges.

The ‘rms-error’ is a measure of the deviation of the actual from the desired shape change. The desired shape change is specified in terms of the vertical

displacement of twenty points on the wing skin, arranged in two rows of ten (see the output points shown in Fig. 2). The reason for the two rows is to ensure there is no substantial variation of deflection in the spanwise direction. The desired shape change is equivalent to the vertical deflection that would result if the leading edge is rotated by 5º downwards, and is shown in Fig. 9.

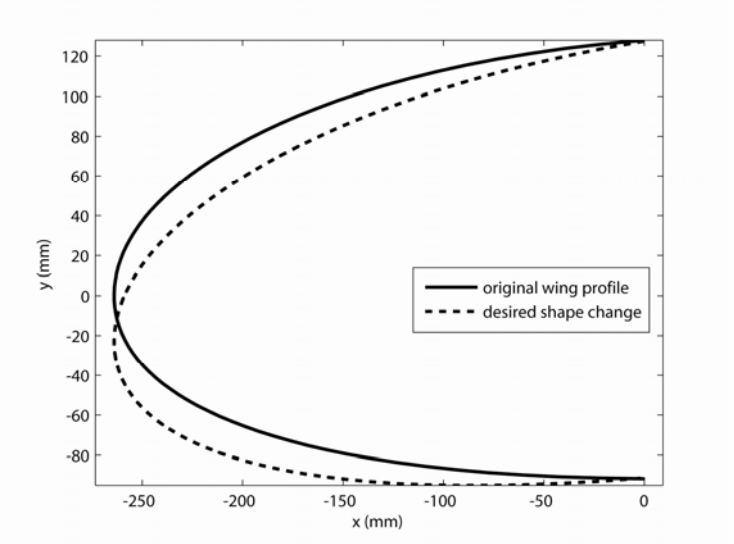

Fig. 9 Desired wing profile shape change

4.2 RESULTING TOPOLOGY

Following 3000 iterations of the optimisation algorithm the topology shown in Fig. 10 was generated. Under actuation, the rms error of the actual versus the desired shape change is less than 1 mm, although the peak stress is 1353 MPa, which is significantly higher than the yield stress defined in Table 1. This response is shown in Fig. 11. It should be noted that although the structure appears two-dimensional, it is in fact three-dimensional and contains the wing skin. This is evident from the deflected shape where it can be seen that the deflection is not completely uniform in the spanwise direction. The result is encouraging however, as it represents a preliminary solution to a problem that would have been difficult to solve by a more conventional design process, and which satisfies the constraints that were prescribed. It is also a structural form which, as it contains no member cross-overs, is feasible to be constructed.

Clearly, however, it is necessary to modify the structure before a physical model can be fabricated in order to ensure that the yield stress of the material is not exceeded.

5 MANUAL MODIFICATION

This section describes modifications to the design produced by the first optimisation attempt which are made manually and which result in a design that is physically possible.

5.1 NONLINEAR ANALYSIS

The first stage of the modification is to confirm that the linear analysis used in the optimisation is valid. This is carried out by running a fully-nonlinear MECANO

analysis and comparing the results with the earlier linear-analysis results. To account for the possibility that individual members may buckle, an arc-length analysis (requested by the CONT 1 variable in the .SUB command) is used.

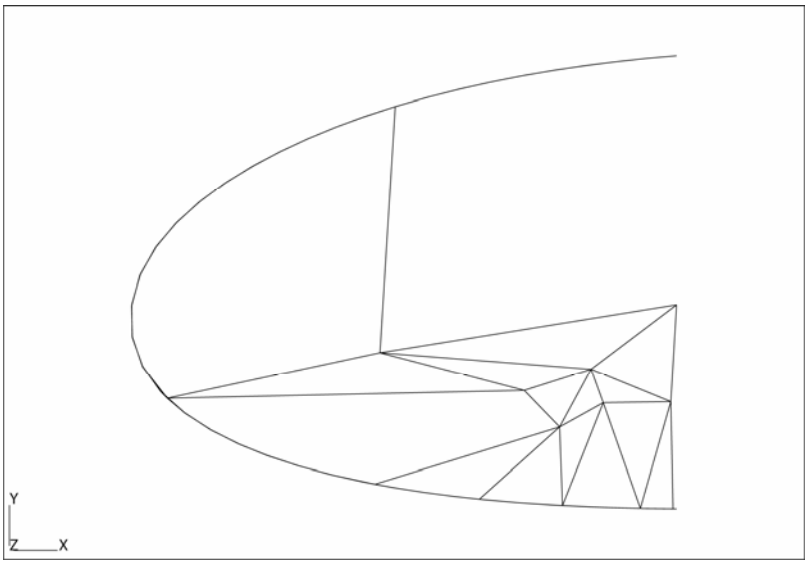

Fig. 10 Initial optimised compliant wing structure

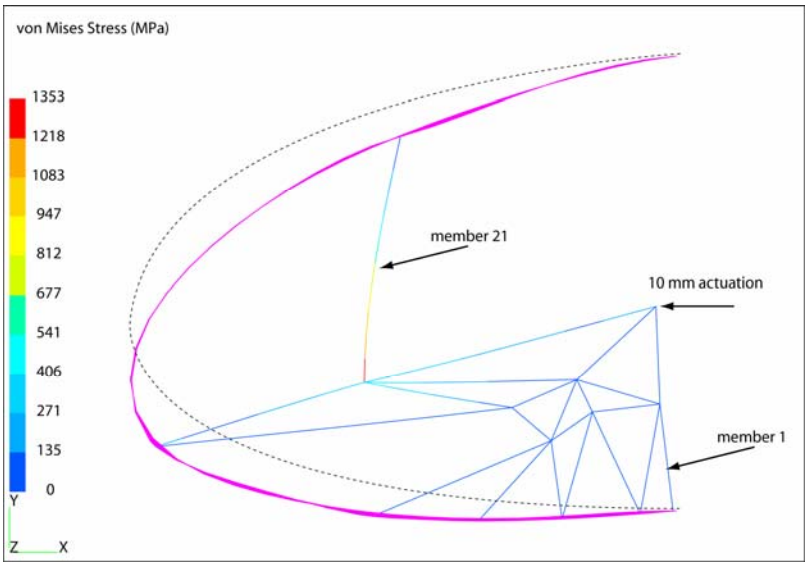

Fig. 11 Peak stress and shape change resulting from actuation of the initially optimised structure

It was found that for the design proposed by the optimisation analysis, buckling did not occur (so the linear analysis used by the optimisation was valid), and that the peak stresses occurred within the rib structure. The next stage of modification is to insert hinges at the ends of members where high bending moments currently result in excessive stress. Inspection of the beam bending moment diagrams, for the rib structure members showed that large bending moments occur throughout member 21 (see Fig. 11), and at the connection between member 1 and the rib-skin connection strip. Additionally, member 21 is subjected to a low amount of tension when the

structure is actuated. This indicates that if the connections at both ends of member 21 are replaced with hinges they may readily be implemented as localised compliant hinges.

The high bending moment in member 1 is dealt with by removing the member in its entirety. This changes the topology. It may be reasoned that, if stress had been constrained in the original analysis, the optimisation process would have resulted in the highly stressed member being removed.

These modifications are seen to reduce the peak stress to acceptable levels. In addition, as the stresses in the wing skin are not high, it is removed leaving just the connection strip. Also, the aerodynamic loading is not applied. This is to enable the design of a demonstration model, which is described in more detail in the following section. Following these modifications, the stress was reduced to 139 MPa – substantially less than the material yield stress.

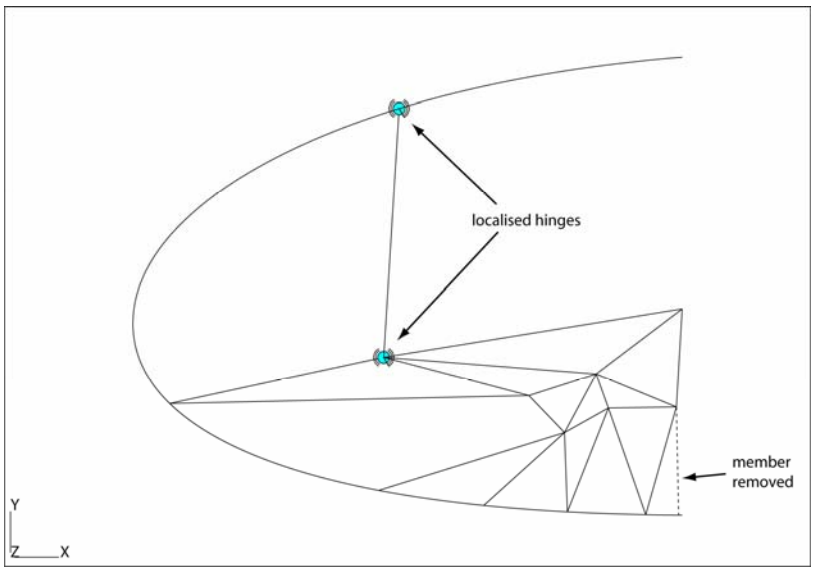

Fig. 12 Optimised structure, manually modified to reduce peak stress

5.2 ANALYSIS OF A DEMONSTRATION MODEL

In this section the final steps that were taken to enable the construction of a model to demonstrate the general functionality of the compliant structure are described. The first is to reduce the peak actuation displacement. The reason for this is, as can be seen in Fig. 13, there is a region of increased displacement on the upper surface of the wing resulting from the absence of aerodynamic loading. This loading causes an upward suction on the top surface of the wing which results in a reduced downward deflection under actuation. Therefore, in the absence of this aerodynamic loading a reduced actuation displacement results in the desired shape change.

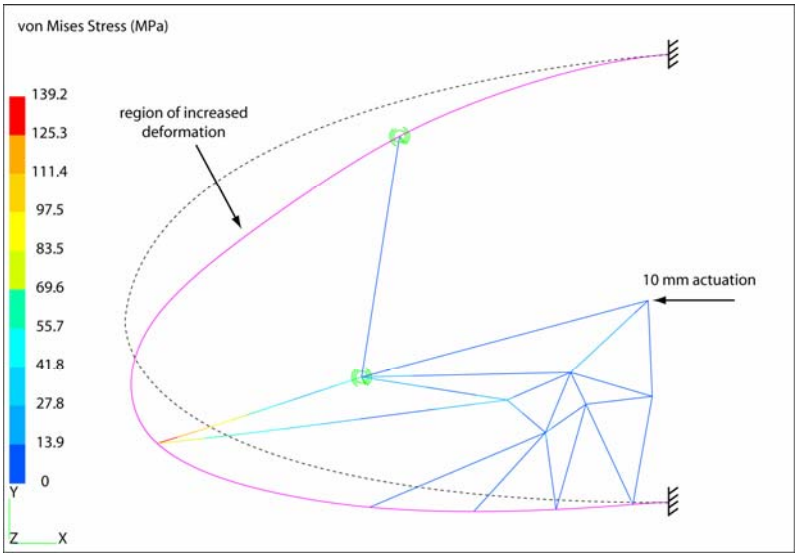

Fig. 13 Peak stress and shape change of manually-modified structure

Finally, a solid finite element model was created to enable the stress concentrations introduced by the physical realisation of the beams and compliant hinges to be accounted for, and the design modified by rounding all the sharp corners accordingly. This design is shown in Fig. 14. It can be seen that, under actuation, a shape change very similar to the desired change shown in Fig. 9 is produced without resulting in excessive material stresses. This is the final step in the process of converting the structure suggested by the topology optimisation into a feasible design. A full-size physical model of the manually modified structure is shown in Fig. 15.

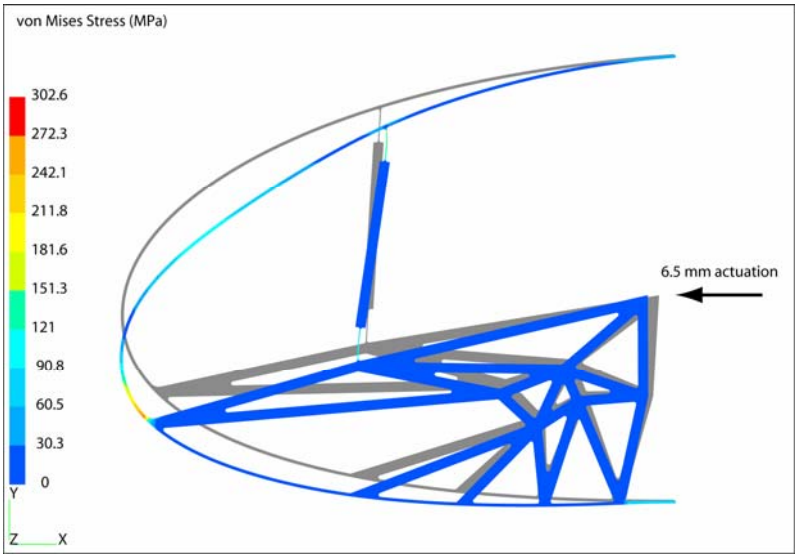

Fig. 14 Peak stress and deformed shape under actuation of a solid model of the manually-modified structure

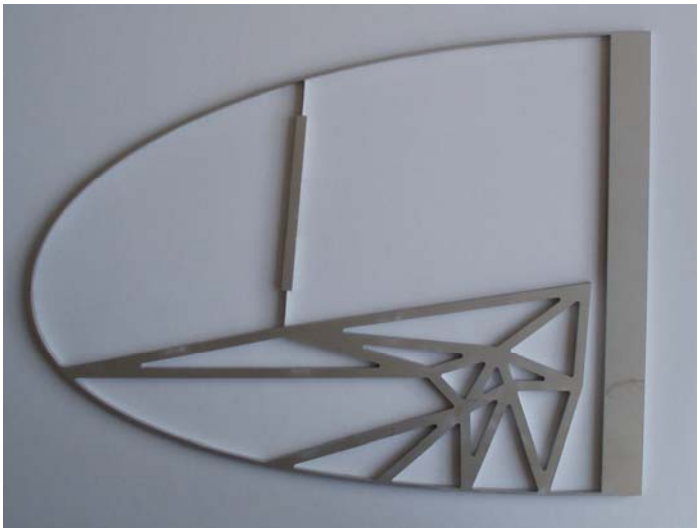

Fig. 15 Physical model of the manually-modified structure

6 OPTIMISATION EXTENSION

It has been demonstrated how a design generated by a simplified topology optimisation can be refined manually to produce a feasible design. In this section, it is briefly investigated what effects the increase in complexity of the optimisation problem definition has on the output solution.

In addition to the variability of the control point locations and the existence of load paths permitted in the initial optimisation, the rib member thickness is also included. Additionally, the optimisation software is allowed to choose the type of member end-connection. This entails an alteration in the definition of the 'model-complexity' objective function. In this case it is extended to the sum of the number of load paths and the number of hinges. Simpler designs contain fewer localised hinges, as their implementation as living hinges cannot be adequately included in the synthesis stage of the design. Finally a constraint limiting the peak stress under actuation to 280 MPa (providing a 30% margin against yield) is included.

The optimisation has been seen to converge to realistic solutions. However, it is clear that further measures must be taken to ensure that feasible structures are generated, as currently localised hinges may be specified in confined areas and at the end of members subjected to large compressive forces. Also, it is not sufficient just to remove the possibility of member cross-over, as restrictions must also be placed on the angle between adjacent members. Finding an implementation of this limitation that is suitable for the optimisation routine will be the subject of further work.

At the current time, fully-nonlinear analysis has not been made available to the optimisation. This is due to the currently unacceptable increase in computation time required. However, it does mean that currently it is necessary to ensure that there is no local buckling subsequent to the proposal of a design by the optimisation, as local buckling can result in substantially increased stresses which would not be indicated by a linearised analysis.

7 CONCLUSIONS

This paper has shown that, using the current functionality of SAMCEF and BOSS-quattro, it is possible to carry out a topological and geometrical optimisation of lattice-based compliant structures. These structures may have distributed- or

concentrated-compliance, or a combination of the two. Special attention has also been focussed on the generation of structures which are not only mathematically- but also physically-feasible. It is hoped that the general methods presented above may be used and extended to enable the synthesis of structures for many alternative problems.

It may be concluded that one of the primary reasons that SAMCEF is well suited to this topological optimisation is due to the availability of logical flow within the command language. Without the ability to switch between load-path combinations and member connection types (inter alia) provided by this functionality, the variation of structural topology by the optimisation would not be possible.

In addition, the use of commercially-available software means that the technique may be readily extended. This may include the use of: fully-nonlinear analysis (as discussed above); the use of additional element types, for example solid elements; additional loading types, such as thermal loading; further connection types, such as prismatic joints; and many more.

ACKNOWLEDGEMENTS

The authors would like to express their gratitude to Ettore Baldassin, Aurelio Boscarino, and Giovanni Carossa of Alenia-Aeronautica, and Fréderic Cugnon and Philippe Andry of Samtech for their valuable assistance and collaboration with the work presented in this paper. This work was carried out within the SYNCOMECS project, funded under the Sixth Framework Programme of the European Commission.

REFERENCES

[1] HOWELL, L. (2001) *Compliant Mechanisms* John Wiley and Sons

[2] KOTA, S., HETRICK, J. and OSBORN, R. (2006) *Adaptive Structures: Moving into the Mainstream* Aerospace America, AIAA, 9, pp. 16-18

[3] LU, K.-J. and KOTA, S. (2003) *Design of Compliant Mechanisms for Morphing Structural Shapes* Journal of Intelligent Material Systems and Structures, 14, pp. 379-391

[4] LU, K.-J. and KOTA, S. (2005) *An Effective Method of Synthesizing Compliant Adaptive Structures using Load Path Representation* Journal of Intelligent Material Systems and Structures, 16, pp. 307-317

[5] PEDERSEN, C., BUHL, T. and SIGMUND, O. (2001) *Topology Synthesis of Large-displacement Compliant Mechanisms* International Journal for Numerical Methods in Engineering, 50, pp. 2683-2705